Temperature-Responsive Self-Assembled Monolayers of Oligo(ethylene glycol): Control of Biomolecular Recognition

Hadi M. Zareie,[†,*] Cyrille Boyer,[‡] Volga Bulmus,[‡,§,*] Ebrahim Nateghi,[†] and Thomas P. Davis[‡]

[†]Institute for Nanoscale Technology, University of Technology, Sydney (UTS), Sydney 2007, Australia, [‡]Centre for Advanced Macromolecular Design (CAMD), School of Chemical Sciences and Engineering, and [§]School of Biotechnology and Biomolecular Sciences (BABS), The University of New South Wales (UNSW), Sydney 2034, NSW Australia

ABSTRACT Self-assembled monolayers (SAMs) of oligo(ethylene glycol) (OEG)-tethered molecules on gold are important for various biorelevant applications ranging from biomaterials to bioanalytical devices, where surface resistance to nonspecific protein adsorption is needed. Incorporation of a stimuli-responsive character to the OEG SAMs enables the creation of nonfouling surfaces with switchable functionality. Here we present an OEG-derived structure that is highly responsive to temperature changes in the vicinity of the physiological temperature, 37 °C. The temperature-responsive solution behavior of this new compound was demonstrated by UV—vis and nuclear magnetic resonance spectroscopy. Its chemisorption onto gold(111), and the retention of responsive behavior after chemisorption have been demonstrated by surface plasmon resonance (SPR), X-ray photoelectron spectroscopy (XPS), and atomic force and scanning tunneling microscopy. The OEG-derived SAMs have been shown to reversibly switch the wettability of the surface, as determined by contact angle measurements. More importantly, SPR and AFM studies showed that the OEG SAMs can be utilized to control the affinity binding of streptavidin to the biotin-tethered surface in a temperature-dependent manner while still offering the nonspecific protein-resistance to the surface.

KEYWORDS: oligo(ethylene glycol) · self-assembled monolayer · temperature-responsive · responsive surfaces · nonfouling; · biosensor

Self-assembled monolayers (SAMs) of oligo(ethylene glycol) (OEG)-tethered molecules on gold are important for various biorelevant applications such as biomaterials and bioanalytical devices.[1–5] Thin films of OEG ($n \geq 3$) have proven to prevent the nonspecific protein adsorption from biological media.[5–22] OEG's unique hydration feature, that is, a tightly bound layer of interphase water, prevents direct contact with proteins, which results in resistance to the adsorption of proteins.[23,24] It is well-known that the interaction of poly(ethylene glycol) (PEG)s with water depends on temperature.[25,26] The solubility of PEG chains decreases with increasing temperature, leading to a decreased hydration state followed by the phase separation of the chains at elevated temperatures. Although it decreases with increasing chain length, the phase separation temperature of PEG is typically above 100 °C.[27]

Self-assembly of stimuli-responsive molecules should enable the generation of well-defined interfaces with switchable functionality with potential uses in biomedical and nanobiotechnology applications.[28–40] As OEG is the most widely used material to create protein-resistant interfaces, its use as a temperature-responsive switch, while keeping its protein-resistant feature, would be desirable to create inert but "smart" gold-biofluid interfaces for numerous applications.

Here we describe temperature-responsive SAMs of a new OEG derivative that can be used to control the affinity binding of streptavidin to biotinylated surfaces in a temperature-dependent manner while providing a nonspecific adsorption-resistant feature. The temperature-responsive solution behavior of the OEG derivative, its chemisorption onto gold(111), and the retention of responsive behavior after chemisorption have been demonstrated. The OEG-derived SAMs have been shown to reversibly switch the wettability of the surface and more importantly control the binding of streptavidin to the biotin-tethered surface in a temperature-dependent manner.

OEG with twelve repeating ethylene glycol units (the number average molecular weight, $M_n = 500$ g/mol; degree of polymerization, $n = 12$ units; polydispersity index, PDI = 1.04) was modified to include a pyridyldisulfide end group adapting a procedure reported earlier[41] (Figure 1a and Supporting Information Figure S1). The temperature-responsive solution behavior of the disulfide-linked OEG derivative (PEG12) is shown in Figure 1b. A sharp increase in the visible light absorption of the PEG12 solution upon heating indicated a

*Address correspondence to hadi.zareie@uts.edu.au, vbulmus@unsw.edu.au.

Received for review February 7, 2008 and accepted March 25, 2008.

Published online April 4, 2008.
10.1021/nn800076h CCC: $40.75

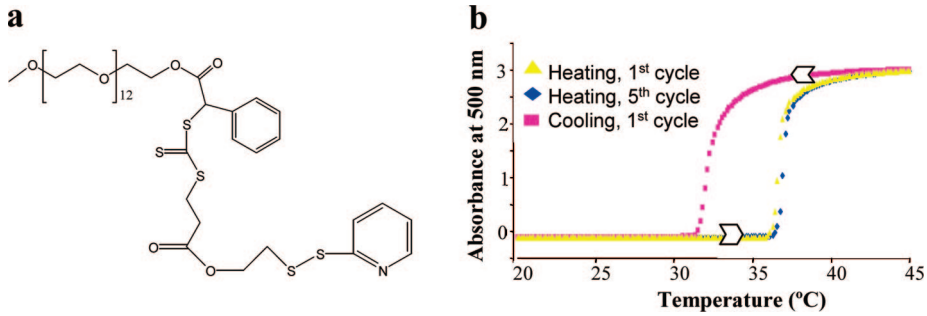

Figure 1. Chemical structure and temperature-responsive solution behavior of PEG12: (a) chemical structure; (b) change in the absorbance of PEG12 solution (0.2 mg/ml in distilled water) upon heating and cooling. Two different heating curves are from the first and fifth heating cycle. The optical path length of the spectrometer cell is 1 cm.

lower critical solution temperature (LCST) of 37 ± 0.5 °C. During twenty-times repeated heating and cooling cycles from 25 to 45 °C, the same LCST and the same phase transition profile were observed indicating that the phase transition of the polymer was reversible. There was a difference of ca. 8 °C in the phase transition obtained upon heating and cooling of the same solution. Similar behavior was previously reported for other temperature-responsive polymers.[42] The temperature-responsive behavior of OEG derivatives with two different numbers of ethylene glycol repeating units (n = 8 and 16) was also investigated. With the small change in the number of ethylene glycol units, the LCST changed significantly (~30 °C) (Supporting Information Figure S2). ^{1}H NMR analysis of PEG12 in deuterium oxide (Supporting Information Figure S3) revealed the decrease in the ratio of the integration of ethylene glycol unit protons ($\delta \approx 3.6$ ppm) to the integration of methylene ester protons ($\delta \approx 4.0$ ppm) upon heating (above 40 °C), which indicated the decrease in the interactions between ethylene glycol units and water above the LCST.

From the above-mentioned observations, it is clear that the modification of oligo(ethyleneglycol) with phenyl-methyl-trithiocarbonyl-propionic acid 2-dithiopyridyl-ethyl ester decreases the overall hydrophilicity significantly. The addition of hydrophobic units such as phenyl and thiocarbonyl to the OEG structure makes the phase transition of the compound to occur at temperatures lower than the transition temperature of the nonmodified OEG (*i.e.*, above 100 °C).[43–47] For an OEG with no modification, while the temperature increase at slightly above the ambient temperatures decreases slightly the solubility of OEG, the decrease is not sufficient to cause the phase separation of the chains. However, when there are hydrophobic groups attached to the OEG structure, the relatively more hydrophobic character of the overall structure facilitates the phase-separation upon decrease in the solubility of OEG units at increasing temperatures.

Surface plasmon resonance (SPR) measurements of the adsorption of PEG12 solution onto a bare gold (Au) surface showed a surface coverage[48] of ~473.4 ng/cm^2 (~2.8 × 10^{14} PEG12/cm^2) and an average surface thickness[49] of ~4.97 nm indicating a monolayer of PEG12 (Figure 2). A control SPR experiment using PEG12 without pyridyldisulfide groups showed no measurable SPR shift suggesting that the pyridyldisulfide group is required for the adsorption of PEG12 to the gold surface (Supporting Information, Figure S4).

XPS revealed the chemisorbed PEG12 on Au(111) (Figure 3 and Supporting Information Figures S5−S7). In Figure 3a, the peak positions on the S2p spectrum of the disulfide-linked PEG12 on Au suggested the presence of the −C−S−, −C═S and/or −S−Au bonds on the surface. When the relative intensity of the peaks at 161.6 eV (−C═S and/or −S−Au bonds) and 163.5 eV (−C−S− bond) was compared between the S2p spectra of PEG12 on gold and alumina (Figure 3a and 3b), the intensity ratio of the peak at 161.6 eV to the peak at 163.5 eV was found to be higher on the gold surface. This clearly revealed the formation of a −S−Au bond between PEG12 and the surface.[49,51] The intensity ratio of the peak at 161.6 eV to the peak at 162.8 eV in Figure 3a (top spectrum) was lower than the expected fixed ratio of 1:2 of S2p1/2 and S2p3/2 components. This was attributed to the overlapping of the S2p3/2 binding energy of −C═S bond with the S2p1/2 binding energy of a −S−Au bond. The presence of the peaks at binding energies between 167.8 and 169.0 eV in Figure 3a was attributed to several overlapping doublets of oxidized sulfur species, that is, sulfate.[51] From the XPS spectra in Figure 3a (S2p, C1s and O1s), the theoretical and the experimental composition of the surface after the chemisorption of PEG12 were found to be in good agreement (Supporting Information, Table S1). Identification of S2p binding energies of a −S−Au bond at 161.6 eV (162.8 eV for p1/2) from a

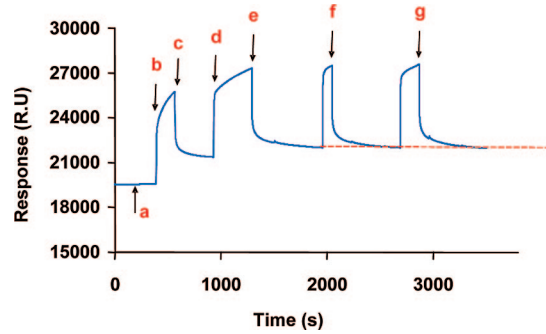

Figure 2. SPR analysis of PEG12 chemisorption on Au. Arrows show injections of (a) nanopure water, (b and d) PEG12 solution, (c and e) nanopure water, (f and g) repeat of PEG12 solution and water rinse.

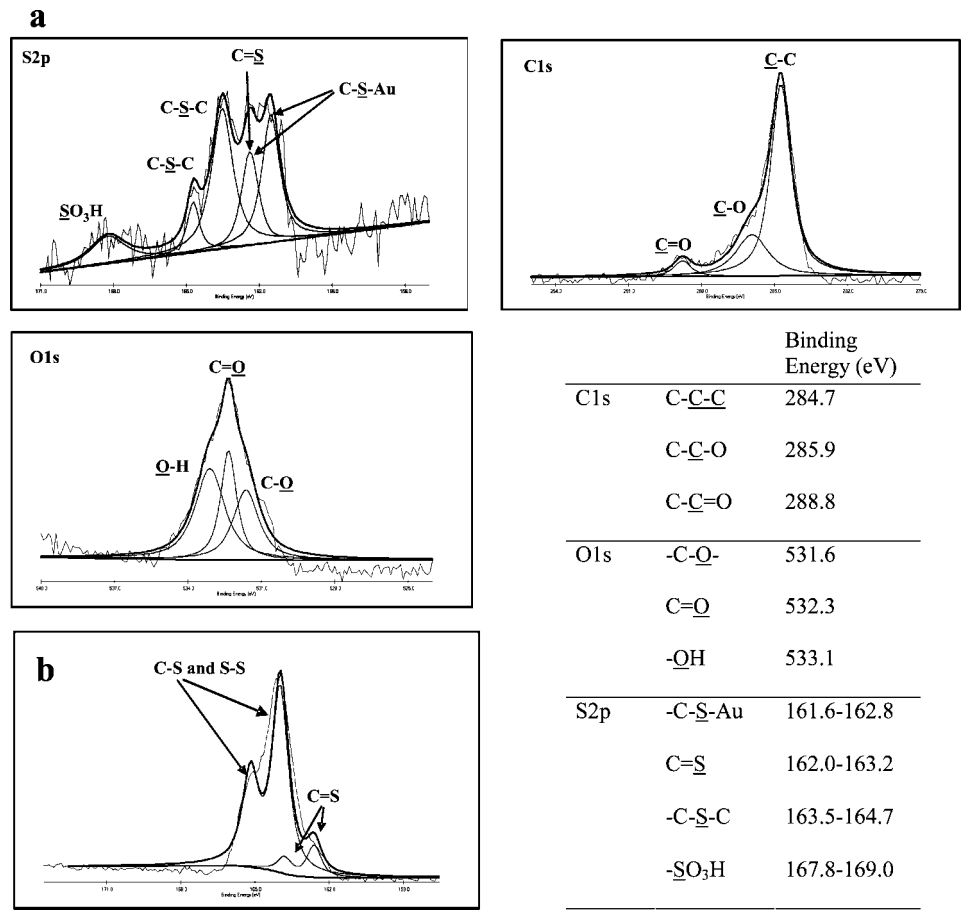

		Binding Energy (eV)
C1s	C-C-C	284.7
	C-C-O	285.9
	C-C=O	288.8
O1s	-C-O-	531.6
	C=O	532.3
	-OH	533.1
S2p	-C-S-Au	161.6-162.8
	C=S	162.0-163.2
	-C-S-C	163.5-164.7
	-SO_3H	167.8-169.0

Figure 3. (a) XPS S2p, O1s, and C1s spectra of PEG12 assembled Au(111) surface and the binding energy values obtained from the spectra; (b) S2p spectrum of PEG12 on alumina.

control XPS experiment (Supporting Information, Figure S5) testing the chemisorption of hydroxyethylpridyldisulfide onto the gold substrate showed that the chemisorption of pyridyldisulfide compound to Au occurs through the cleavage of the disulfide bond, supporting the previous findings by others.[48–53] In another control XPS experiment (Supporting Information Figures S6 and S7), the PEG12 compound without a pyridyldisulfide group, showed insignificant chemisorption to Au(111), supporting the above-mentioned SPR results and also indicating that the trithiocarbonate (−S−(C═S)−S−) is not the responsible group for the chemisorption of the disulfide-linked PEG12 to Au. In summary, combination of the XPS results of the PEG12 assembled Au(111) surface and the control experiments (PEG12 derivative without a pyridyldisulfide group on Au(111) and alumina, and a model compound, hydroxyethylpridyldisulfide assembly on Au(111) and alumina) revealed that (1) the pyridyldisulfide group is necessary for the chemisorption of PEG12 to Au(111), (2) the trithiocarbonate (−S−(C═S)−S−) group is not responsible for the chemisorption, (3) chemisorption occurs through the cleavage of the disulfide bond of the pyridyldisulfide group yielding the thiolate form of the compound attaching to Au *via* formation of a −S−Au bond.[48–51]

Figure 4a shows a typical AFM image of the assembly of PEG12 on Au(111). From the AFM image, the PEG12 layer on the Au islands could be clearly observed. Line profiles across the surface etched by the AFM tip revealed a height of ~5 nm, which was in good agree-

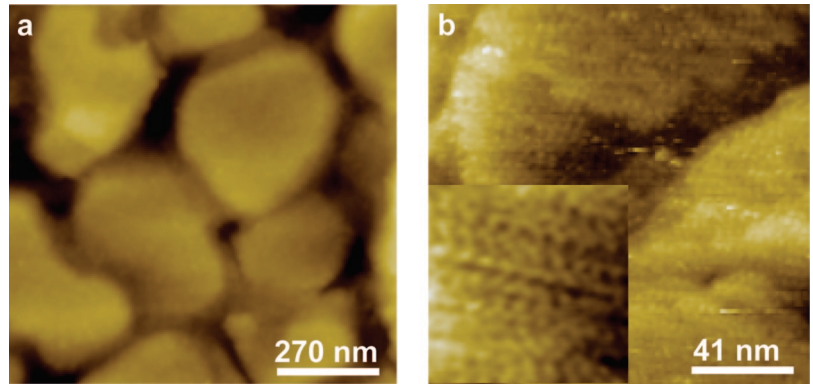

Figure 4. (a) AFM and (b) STM images of PEG12 assembly on Au(111), respectively. The inset in panel b represents the higher magnification image at 30 × 30 nm. Images are raw data except for the inset, which is contrast-enhanced and slightly low pass filtered to accentuate molecular features.

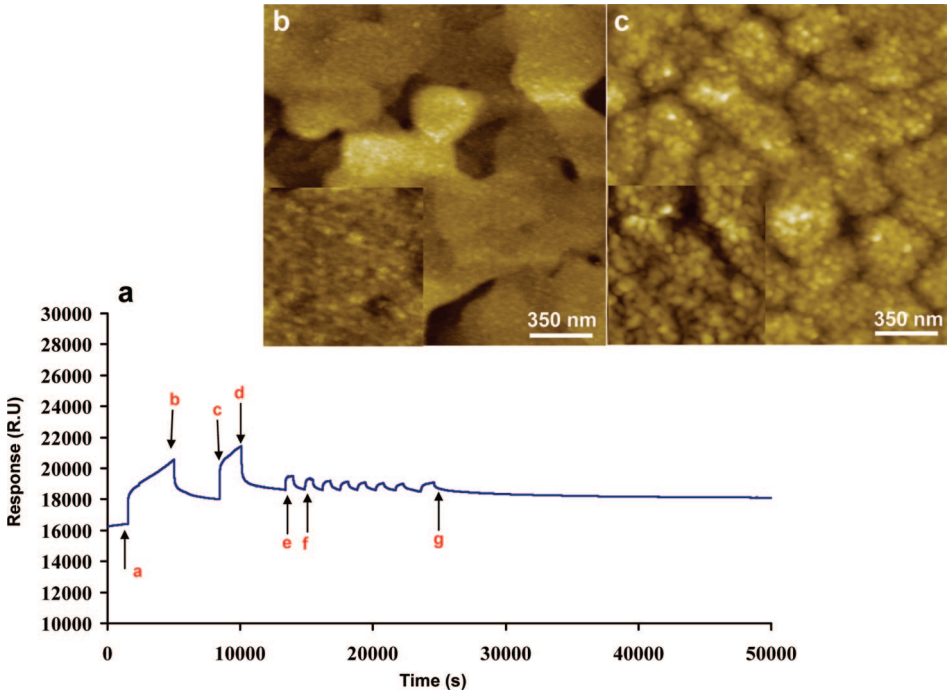

Figure 5. Temperature responsive behavior of PEG12 on Au substrates by SPR and AFM. (a) SPR sensogram: The arrows show (a−d) two injections of PEG12 solution and subsequent rinses with water and (e−g) eight injections of water at 45 °C. (b and c) AFM image of Au(111) substrate with *in situ* assembled PEG12 after injection of water at 23 and 45 °C, respectively.

ment with a single layer of bound PEG12 (Supporting Information, Figure S8). The STM image (Figure 4b) showed features of approximately 0.9 ± 0.1 nm diameter, which were consistent with individual PEG12 molecules. Thus, AFM and STM measurements confirmed also the presence of a monolayer of PEG12 on Au(111) surface, supporting the SPR results obtained.

The SPR sensogram (Figure 5a) of the PEG12 film showed rapid shifts in RU upon heating (45 °C) and cooling (23 °C), which was possibly due to the change in the refractive index and film thickness during the temperature-dependent phase transition and collapse of PEG12 chains. During eight repeating heating and cooling cycles, the same SPR profile was observed. A gradual decrease in the RU difference upon repetitive heating−cooling cycles was also observed. Since there was no indication of the loss of the temperature sensitivity during 20-times repeated heating−cooling cycles as determined by the turbidity measurements of the PEG12 solutions, the gradual decrease in the RU difference was attributed to the possible several effects such as the incomplete conformational transition of the PEG chains from a previous heating−cooling cycle and the changes in the orientation of the chains upon phase transition. Injection of water at 45 °C to the bare substrate (that does not have PEG12 assembly) did not cause any detectable changes in the SPR response (Supporting Information, Figure S9).

The AFM analysis of the *in situ* assembled PEG12 revealed that the rodlike morphology of the PEG12 molecules at room temperature (Figure 5b) changed to globular features at 45 °C (Figure 5c). The line profiles taken along the PEG layer before and after heating indicated a decrease in the height of the PEG12 layer upon heating (Supporting Information Figure S11). This was attributed to the conformation change of PEG12 chains on the surface from an extended to a collapsed state.[23,35]

The water contact angle (θ) of the PEG12 assembled on Au(111) increased from 44 to 70° upon heating from 25 to 45 °C (Figure 6a), indicating the transition from a hydrophilic to a hydrophobic state.[54,55] The transition from hydrophilic to hydrophobic state was reversible (*i.e.*, upon cooling from 45 to 25 °C, the contact angle went back from 70 to ∼45°). The contact angle change of the surface with increasing temperatures (Figure 6b) showed a profile similar to that of phase transition of PEG12 solution observed by UV−vis spectrometer (Figure 1). The change in the surface hydrophilicity with temperature was attributed to the temperature-responsive behavior of the PEG12 assembly on the surface. As determined by the UV−vis and NMR spectrometer analysis of PEG12 solution (discussed previously in the text), the interaction of PEG12 with water decreases with the increase in the temperature, which is driven by the entropy. The temperature-dependent decrease in the water binding capacity of PEG12 is expected to lead to the decrease in the hydrophilicity of the surface onto which PEG12 molecules are chemisorbed. The retention of the temperature-responsive behavior of PEG12 after chemisorption onto a gold surface suggests that the phenyl-trithiocarbonyl group attached to the OEG chain provides a nonpolar microenvironment to OEG units sufficient enough to cause the phase separation of the overall structure chemisorbed onto the surface at slightly elevated temperatures. It also indicates that the absence of a thio-pyridine group does not affect significantly the responsive-behavior of the overall structure. Also, the temperature at which the contact angle started increasing (∼40 °C) was observed to be slightly higher than the temperature at which the PEG12 solution turned to cloudy (∼37 °C). The phase-separation of PEG12 molecules in solution results from the combined effect of the intrinsic collapse of the individual molecules be-

cause of the increased intramolecular interactions and subsequent aggregation tendency *via* increasing hydrophobic interactions. Therefore, the temperature at which the phase-separation is observed in solution is dependent on the concentration of the solution. However, the phase-separation of the chemisorbed PEG12 occurs only through the collapse of individual molecules. Considering this, the higher temperature observed for the phase separation of chemisorbed PEG12 is expected.

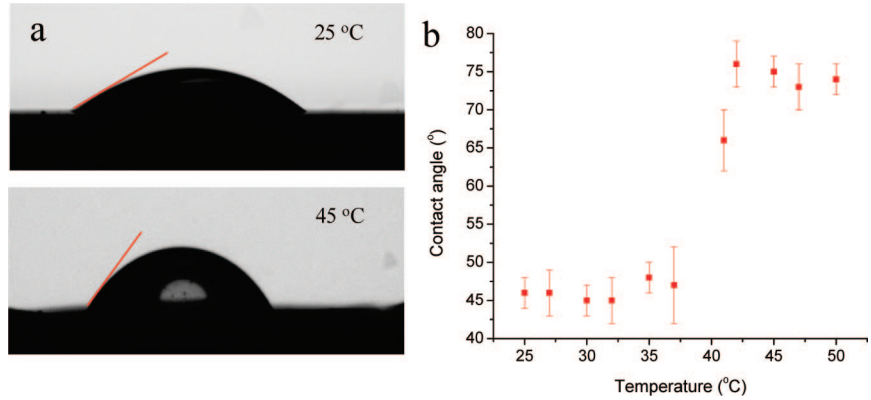

Figure 6. Measurement of water contact angle on a PEG12 assembled Au(111) surface: (a) picture of water drop at varying temperatures; (b) evolution of contact angle with increasing temperature. Each value is an average of 5 different measurements. Bars represent the deviation of 5 different measurements from the average value.

The potential of PEG12 SAMs to offer a protein-resistant interface with a temperature controlled function was illustrated by a model study in which temperature-dependent streptavidin immobilization onto a mixed SAM of PEG12 and a biotinylated disulfide (Ez-link) was investigated (Figure 7a−c). The biotin containing component of the mixed SAM, that is, Ez-link, was chosen because of its molecular length (theoretical: ~3 nm) that is *ca.* 53% of the length of PEG12 in extended conformation (theoretical: ~5.7 nm). In the mixed SAM, PEG12 molecules on the surface is expected to be diluted with Ez-link molecules at an estimated PEG12/Ez-link mol ratio of ~2:1 considering the previous reports on the commonly used mixed SAMs of biotinylated and OEG terminated alkanethiols.[56,57] In the mixed SAM at room temperature, the biotin molecules are expected to be embedded in the PEG12 layer owing to the length difference between the two components, that is, PEG12 and Ez-link. When the temperature is increased to 45 °C, PEG12 molecules, the temperature-responsive component of the mixed SAM, are expected to collapse as a result of the increased hydrophobic intrachain interactions which leads to the condensation of the individual chains (*i.e.*, shrinkage in the hydrodynamic diameter and hence in the film thickness of PEG12 molecules). This may reveal the biotin molecules tethered to the non-temperature sensitive component of the mixed SAM on the surface at 45 °C. Indeed, SPR measurement (Figure 7d) showed that the adsorption of SA to the mixed SAMs increased ~29-fold when the temperature was increased from 23 to 45 °C (surface coverage of SA: *ca.* 3.2 and 91 ng/cm^2 at 23 and 45 °C, respectively). The increase in the adsorption of SA at high temperature was attributed to the increased availability of biotin molecules upon the collapse of neighboring PEG12 chains at temperatures above the phase transition temperature of PEG 12 molecules. The SA coverage of 91 ng/cm^2 indicated a biotin/SA ratio of ~97 on the surface, assuming a monolayer with 32 mol % Ez-Link.[56−59] Similar ratios were reported in the literature[59,60] for the binding of SA to the commonly used (nonresponsive) mixed SAMs of biotinylated and OEG terminated alkanethiols. The good agreement between the experimental SA coverage obtained using mixed SAMs of PEG12 (at 45 °C) and the coverage values reported in the literature for the commonly used non-responsive mixed SAMs suggested that the collapse of PEG12 molecules was efficient to expose the biotin molecules on the surface to SA. Control SPR experiments performed using pure SAMs of PEG12 only (not mixed with Ez-link) showed RU shifts around the detection limit of the SPR instrument (10 RU), indicating a nonspecific binding of approximately 1 ng SA/cm^2 to PEG12 layer at both 23 and 45 °C (Supporting Information Figure S12). This shows that the protein-resistant character of PEG12 is not affected significantly by the increase in the temperature in the studied range. This finding supported, to some extent, previous reports by Grunze and co-workers[60] and Whitesides and co-workers.[6]

The corresponding tapping mode liquid phase AFM images (Figure 7e and f) of the mixed SAMs of PEG12 and Ez-link after incubation with SA at 45 °C showed clearly the coverage of the surface by SA molecules.[59,60] The average apparent diameter of the SA molecules measured from AFM images was ~9 nm. A number density of ~1.9 × 10^{10}/cm^2 was obtained by counting bright spots on the AFM image, which was *ca.* 45-fold less than the density calculated from the SPR response (9.2 × 10^{11} SA/cm^2), indicating that the bright spots might comprise the cluster of SA molecules. Here, it should be noted that the temperature-dependent denaturation and conformational changes in SA occur above 70 °C,[61−63] which excludes the possibility of clustering of SA molecules on the surface at 45 °C due to the denaturation of SA. In addition, the clustering of SA molecules on mixed SAMs has been reported

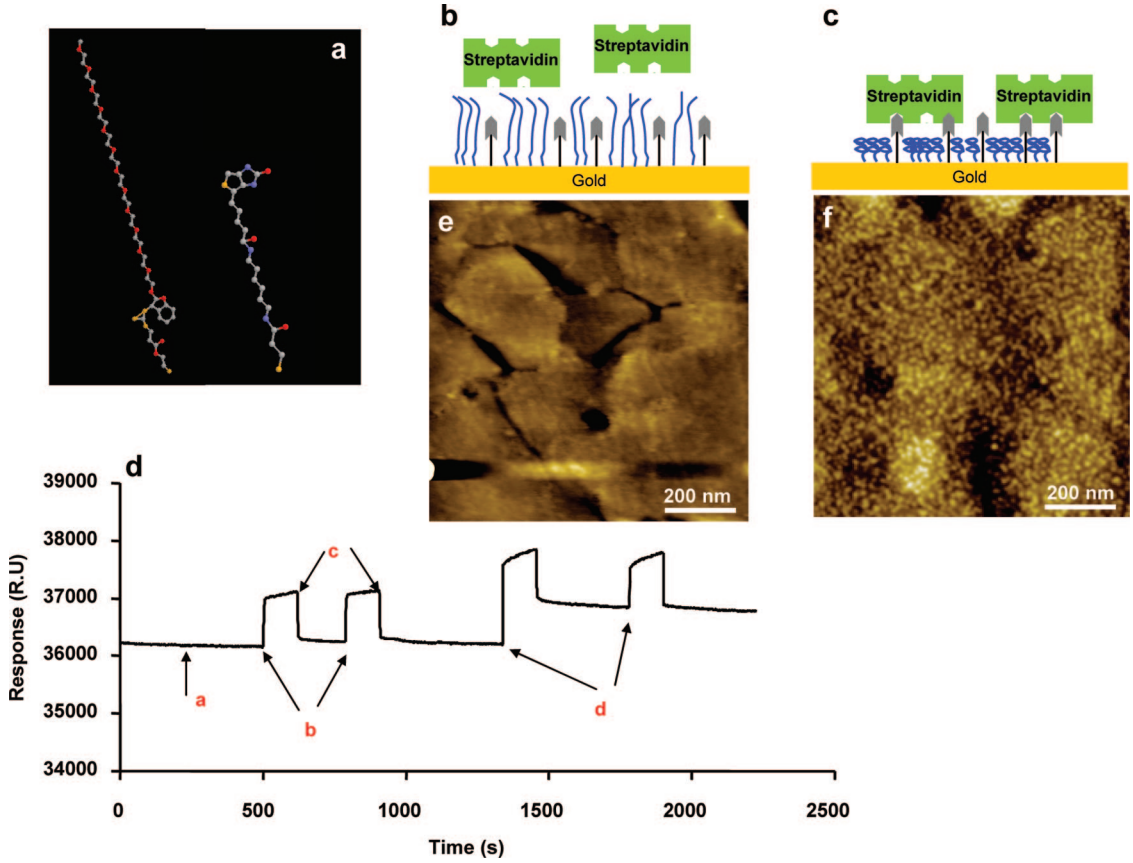

Figure 7. SPR and AFM analyses of SA adsorption onto mixed SAM. (a) Chemical structure of the mixed SAM components; PEG12 (left) and Ez-Link (right); (b and c) schematic representation of SA binding onto mixed SAM at 23 and 45 °C, respectively; (d) SPR sensogram of SA adsorption at 23 and 45 °C. Arrows show injections of (a) water, (b and c) SA solution and water at 23 °C, respectively, (d) SA solution and subsequent water rinse at 45 °C. Panels e and f show the tapping mode AFM images in liquid phase after SA solution injection at 23 and 45 °C, respectively.

previously.[59,60] Considering these, each bright spot on the AFM image, observed at 45 °C was attributed to more than one SA molecule interacted with the Ez-link molecules exposed from the mixed SAM upon the collapse of PEG12 molecules.

In conclusion, we have presented a new OEG-based temperature-responsive compound that can self-assemble onto gold substrate and generate a nonfouling surface that can respond to the environmental temperature changes. We have further shown the potential of the temperature-responsive OEG SAMs for applications, with a model study, by exploiting it to control the affinity interaction of a protein−ligand pair with strong specific affinity in a temperature-controlled way. We believe that the new temperature-responsive, protein-repellent, OEG based SAMs introduced in this manuscript are significant to create "smart" and nonfouling surfaces and can be used in numerous ways for biomedicine, biotechnology, and nanotechnology applications.

METHODS

Materials. All chemicals were used as received, unless otherwise specified. Poly(ethylene glycol) methyl esters (M_n = 750 g/mol, n = 16 units, PDI = 1.05, 98%); (M_n = 500 g/mol, n = 12 units, PDI = 1.04, 98%), (M_n = 350 g/mol, n = 8 units, PDI = 1.05, 98%) were purchased from Fluka. Streptavidin was purchased from Sigma Chemicals Co. and used as received. The SA was dissolved in water at a concentration of 1 mg/mL and stored in Eppendorf tubes in 20 μL aliquots at −20 °C until needed. All water used in the experiment was purified by treatment in a reverse osmosis unit followed by a Millipore unit (18 MW resistivity). *N*-(6-(Biotinamido)hexyl)-3′-(2′-pyridyldithio) propionamide (Ez-link) was purchased from Pierce. Two types of Au(111) were used. One type was Au(111) films (150 nm thick on mica) purchased from Molecular Imaging (Phoenix, AZ) and flame-annealed before use. Second type was homemade Au(111) prepared as described below.

Synthesis of Disulfide-Linked PEGs. The synthesis of pyridyldisulfide linked oligo(ethylene glycol) with 16 repeating unit is described elsewhere.[41] The same compound with 8 and 12 repeating units (PEG8 and PEG12) was synthesized following the same method using oligo(ethylene glycol) (n = 8 and 12) instead of oligo(ethylene glycol) (n = 16). The formation of the final compounds was verified by ^{1}H and ^{13}C NMR, size exclusion chromatography (SEC) and electron spray ionization-mass spectroscopy (ESI-MS). The ^{1}H NMR spectrum of PEG12 is illustrated in the Supporting Information. Chemical structure characteristics of PEG12 are as follows. ^{1}H NMR ($CDCl_3$, 298 K, 300 MHz), δ (ppm from TMS): 2.95 (2H, q, S−CH_2−CH_2), 3.15 (2H, m, −CH_2−$CO_2CH_2CH_2$S−S−), 3.35−3.36 (3H, s, O−CH_3 and 2H, m, −CH_2−$CO_2CH_2CH_2$S−S−)), 3.60 (64H, −O−CH_2−CH_2−O−),

4.25−4.35 (4H, m, $-CO_2-CH_2-$), 5.80 (1H, s, $-CH-S-CS_2$), 7.36 (5H, m, Ar−*H*), 7.1 (1H, m, aromatic hydrogen meta to nitrogen, 7.70 (2H, m, para to nitrogen and ortho to thiol derivatized carbon), 8.45 (1H, q, aromatic hydrogen ortho to nitrogen). ^{13}C NMR, δ (ppm from TMS): 30.50 ($-CH_2-S-(CS)-$), 34.30 ($-CH_2-S-S-$), 37.90 ($S-CH_2-CH_2-(CO)-$), 53.50 ($-CH-S-$), 58.90 ($-O-CH_2-CH_2-O(CO)-$), 60.50 ($-(CO)-O-CH_2-CH_2-S-S$), 70.90 (O-CH_3), 72.30 ($-O-CH_2-$), 127.30, 127.76, 128.80, 129.11, 129.40, 133.21 (*C*H of aromatic group), 119.30, 121.69, 138.10, 149.11, 159.50 (*C*H of pyridyl group), 169.10 and 170.20 (*C*=O), 227.07 (CS_2). ESI-MS of PEG12: $m/z = 1069.4$; theoretical: $m/z = 1069.0$. The number average molecular weight of PEG12, M_n = 1,000 g/mol, PDI = 1.03 (SEC, styrene calibration).

Syntheses of hydroxyethylpyridyl disulfide and PEG12 without a pyridyldisulfide group were reported elsewhere.[41]

Au(111) Preparation for AFM/STM Studies. Freshly cleaved mica samples were cleaned using ethanol and dried using nitrogen gas. Mica samples were placed on a Peltier hot plate inside a vacuum bell jar at 380 °C and 10^{-6} Torr, and left for over 12 h. Gold was then deposited at a rate of 1 Å/s to produce a +100 nm thick film. Samples were left for a further hour and the Peltier heater was turned off. When temperature reached ~30 °C, the chamber was vented with nitrogen. Samples taken from the chamber were immediately hydrogen-flamed. Flame annealing has the potential to remove adsorbed organic impurities and also expands the grain boundaries of the (111) terraces.

Preparation of SAMs. Monolayer structures were prepared by immersing the gold substrates in 1 mM nanopure water or absolute ethanol solutions of PEG12 or PEG12/Ez-link mix (9:1 mol ratio). The container was sealed and incubated for 24−48 h at room temperature. The samples were then washed thoroughly with nanopure water/ethanol and dried using a stream of nitrogen gas.

Size Exclusion Chromatography (SEC). DMAc SEC analysis of the polymers were performed in *N,N*-dimethylacetamide [DMAc; 0.03% w/v LiBr, 0.05% 2, 6-di-butyl-4-methylphenol (BHT)] at 50 °C (flow rate = 1 mL/min) with a Shimadzu modular system comprising an SIL-10AD autoinjector, a Polymer Laboratories 5.0-mm bead-size guard column (50 × 7.8 mm) followed by four linear PL (Styragel) columns (10^5, 10^4, 10^3, and 500 Å) and an RID-10A differential refractive-index detector. The calibration was performed with narrow-polydispersity polystyrene standards ranging from 500 to 10^6 g/mol.

Mass Analysis. Electrospray-ionization mass spectrometry (ESI-MS) experiments were carried out using a Thermo Finnigan LCQ Deca ion trap mass spectrometer (Thermo Finnigan, San Jose, CA). The instrument was calibrated with caffeine, MRFA, and Ultramark 1621 (all from Aldrich) in the mass range 195−1822 Da. All spectra were acquired in positive ion mode over the mass to charge range, m/z, 100−2000 with a spray voltage of 5 kV, a capillary voltage of 44 V, and a capillary temperature of 275 °C. Nitrogen was used as sheath gas while helium was used as auxiliary gas. The sample (1 mg/1 mL) was prepared by dissolution of a 60:40 v/v mixture of THF: methanol with an acetic acid concentration of 0.4 mM. Fifty-six spectra were recorded in positive ion mode with an instrumental resolution of 0.1 Da. All reported molecular weights were calculated *via* the program package CS ChemDraw 6.0 and are monoisotopic. The theoretical molecular weight over charge ratios (m/z, (assuming z) + 1) are calculated using the exact molecular mass of the predominant isotope within the structure.

UV−Visible Spectroscopy. UV−vis spectra were recorded using a CARY 300 spectrophotometer (Bruker) equipped with a temperature controller. The lower critical solution temperature, LCST, was determined at 500 nm. The sample solutions were prepared in distilled water at 0.2 mg/ml (0.2 wt %) concentration. During the measurements, heating and cooling rates were 2 °C/min. The temperature at which 10% of the maximum absorbance of the solution was observed was defined as the LCST.

NMR Spectroscopy. ^1H and ^{13}C NMR spectra were recorded on a Bruker ACF300 (300 MHz) or ACF500 (500 MHz) spectrometer, with D_2O or $CDCl_3$ used as solvents. The solution was equilibrated for 5 min at each set temperature. The data were collected from 25 to 55 °C with 5 °C increments.

Scanning Probe Microscope (SPM). The surfaces were imaged with a Nanoscope III (Digital Instruments, Santa Barbara, CA) atomic force microscope (AFM) apparatus in tapping mode. An AFM liquid cell was utilized to retain the solutions that were injected through plastic tubing. Two different types of experiments were performed. In the first type, Au(111) substrate in deionized water was scanned and then PEG12 solution (1 mM in nanopure water) was injected into the liquid cell, followed by a waiting period of approximately 60 min for *in situ* assembly and rinsing thoroughly with nanopure water. A scan of approximately the same area was then performed. In the second type of experiment, the Au(111) substrate with preassembled PEG12 (as described in preparation of SAMs) was placed in the AFM liquid cell for analysis. The scans were typically done at rates between 1 and 4 Hz. The images were obtained using a silicon nitride cantilever with a nominal force constant of 0.38 N m^{-1}.

For scanning tunneling microscopy (STM), images were acquired using a Nanosurf EasyScan system under ambient conditions. STM piezoelectric scanners were calibrated laterally, with graphite (0001) and Au(111), and vertically, using the height of the Au(111) steps (2.2 Å). The STM tip was prepared from Pt/Ir wire cut under ambient conditions. All images were acquired in a constant-current mode. Typical imaging conditions are bias voltages of 0.5 V and a tunneling current of 3 pA. Images shown are raw data unless stated otherwise. Images were manipulated with the scanning probe image processor (SPIP) software. Contrast-enhanced images were obtained by applying a correlation averaging procedure to analyze repeat molecular units and by applying low-pass filter.

Indentation Experiment to Determine Thin-Film Thickness. Indentation experiments were performed to investigate the thickness of the film. Three indentations were performed using drive amplitude values of 1, 2, and 5 V. The drive amplitude at 5 V showed a significant increase in the force since the depth increased dramatically reaching to the gold surface.

Surface Plasmon Resonance (SPR). The BIACORE K 2000 system from Biacore AB (Uppsala, Sweden) with multiflow cells and internal heating/cooling was used for SPR analyses. In this system, 1000 RU represents adsorption of approximately 1 ng/mm^2.

The Au substrates for SPR studies were purchased from Biacore AB (SIA KIT AU, Sweden). The Au slides were stored under nitrogen. Just prior to use, the gold surfaces were cleaned by immersing the slides in a solution of ammonium hydroxide, hydrogen peroxide, and water (15:15:70) at 60 °C for up to 1 min. The slides were rinsed thoroughly with nanopure water and absolute ethanol before they were dried rapidly with a stream of nitrogen.

For quantitative determination of chemisorption of PEG samples (PEG12: density = 1.12 g/cm^3 (at 20 °C) and 1.10 g/cm^3 (at 45 °C); refractive index = 1.533 at 20 °C and 1.5240 at 45 °C) to gold, the cleaned Au substrates were used as SPR active sensor surface without any further functionalization. For quantitative determination of binding of streptavidin, the cleaned Au substrates were immediately immersed either in a 1 mM solution containing only PEG12 or a mixture of 10 mol % EZ-Link and 90 mol % PEG12 in nanopure water for 24−72 h. After functionalization, the slides were rinsed with nanopure water to remove weakly bound molecules.

SPR experiments were carried out at 10 μl/min flow rate using 1 mM OEG derivatives and 0.2 μM streptavidin solutions in nanopure water.

X-ray Photoelectron Spectrometer (XPS). A Kratos Axis ULTRA XPS incorporating a 165 mm hemispherical electron energy analyzer was used. The incident radiation was monochromatic A1 X-rays (1486.6 eV) at 225 W (15 kV, 15 ma). Survey (wide) scans were taken at an analyzer pass energy of 160 eV and multiplex (narrow) higher resolution scans at 20 eV. Survey scans were carried out over 1200−0 eV binding energy range with 1.0 eV steps and a dwell time of 100 ms. Narrow higher resolution scans were run with 0.2 eV steps and 250 ms dwell time. Base pressure in the analysis chamber was 1.0×10^{-9} Torr and during sample analysis 1.0×10^{-8} Torr. The data were analyzed by the software XPS PEAK. An integral (nonlinear) backgrounds subtraction was used for the treatment of XPS data. The peak shape assumption uses the asymmetric mixed Gaussian−Lorentzian

functions. The peaks assigned use the references48–53, and the book of Beamson *et al.*[64] was used to assign the XPS peaks. PEG12, hydroxyethylpyridyldisulfide, and PEG12 derivative without a pyridyldisulfide group (Supporting Information Figure 10) assembled Au(111) and alumina surfaces were analyzed by XPS.

Contact Angle Measurements. The contacts angles were measured on Au(111) (with or without a PEG12 monolayer) at varying temperatures using the pendant-drop method. The pendant-drop analyses were performed with KSV contact angle CAM 200 (from KSV instruments fitting method Young-Laplace, recording 20 numbers of frames at one frame per second). The pictures were analyzed by Software CAM, optical contact angle and pendant-drop surface tension software V.3.95 (w2k, XP). All measurements were repeated five times.

Acknowledgment. This work was partly supported by the Australian Research Council Discovery Scheme (DP0666689). TPD acknowledges the Federation Fellowship Award of the Australian Research Council. The authors thank Mr. M. Berkahn (Microstructural Analysis Unit at UTS) for training E.N., Institute for Biology of Infectious Disease (IBID, UTS) and Analytical Centre (UNSW) for SPR and NMR/XPS facilities.

Supporting Information Available: Characterization of disulfide linked PEGs (^{1}H NMR, ESI-MS, temperature responsive behavior), SPR sensogram of PEG12 without pyridyldisulfide group on gold, XPS spectrum of PEG12 and hydroxyethylpyridyldisulfide on gold and alumina surface, AFM pictures of PEG12 assembled on Au(111), SPR control experiment for adsorption of SA (Figures S1 to S12, Table S1). This information is available free of charge *via* the Internet at http://pubs.acs.org.

REFERENCES AND NOTES

1. Love, J. C.; Estroff, L. A.; Kriebel, J. K.; Nuzzo, R. G.; Whitesides, G. M. Self-Assembled Monolayers of Thiolates on Metals as a Form of Nanotechnology. *Chem. Rev.* **2005**, *105*, 1103–1169.
2. Nuzzo, R. Biomaterials: Stable Antifouling Surfaces. *Nat. Mater.* **2003**, *2*, 207–208.
3. Bearinger, J. P.; Terrettaz, S.; Michel, R.; Tirelli, N.; Vogel, H.; Textor, M.; Hubbellet, J. A. Chemisorbed Poly(propylene sulphide)-Based Copolymers Resist Biomolecular Interactions. *Nat. Mater.* **2003**, *2*, 259–264.
4. Whitesides, G. M.; Ostuni, E.; Takayama, S.; Jiang, X.; Ingber, D. E. Soft Lithography in Biology and Biochemistry. *Annu. Rev. Biomed. Eng.* **2001**, *3*, 335–373.
5. Prime, K. L.; Whitesides, G. M. Self-assembled Organic Monolayers: Model Systems for Studying Adsorption of Proteins at Surfaces. *Science* **1991**, *252*, 1164–1167.
6. Prime, K. L.; Whitesides, G. M. Adsorption of Proteins onto Surfaces Containing End-Attached Oligo(ethylene oxide): A Model System Using Self-Assembled Monolayers. *J. Am. Chem. Soc.* **1993**, *115*, 10714–10721.
7. Zhen, G. L.; Falconnet, D. E.; Kuennemann, J. V.; Spencer, N. D.; Textor, M.; Zurcher, S. Nitrilotriacetic Acid Functionalized Graft Copolymers: A Polymeric Interface for Selective and Reversible Binding of Histidine-Tagged Proteins. *Adv. Funct. Mater.* **2006**, *16*, 243–251.
8. Lata, S.; Piehler, J. Stable and Functional Immobilization of Histidine-Tagged Proteins *Via* Multivalent Chelator Headgroups on A Molecular Poly(ethylene glycol) Brush. *Anal. Chem.* **2005**, *77*, 1096–1105.
9. Zhen, G.; Eggli, V.; Voeroes, J.; Zammaretti, P.; Textor, M.; Glockshuber, R.; Kuennemann, E. Immobilization Of The Enzyme Beta-Lactamase on Biotin-Derivatized Poly(L-lysine)-g-poly(ethylene glycol)-Coated Sensor Chips: A Study on Oriented Attachment and Surface Activity By Enzyme Kinetics and *in Situ* Optical Sensing. *Langmuir* **2004**, *20*, 10464–10473.
10. Falconnet, D.; Koenig, A.; Assi, F.; Textor, M. A Combined Photolithographic and Molecular-Assembly Approach to Produce Functional Micropatterns for Applications in the Biosciences. *Adv. Funct. Mater.* **2004**, *14*, 749–756.
11. Falconnet, D.; Pasqui, D.; Park, S.; Eckert, R.; Schift, H.; Gobrecht, J.; Barbucci, R.; Textor, M. A Novel Approach to Produce Protein Nanopatterns by Combining Nanoimprint Lithography and Molecular Self-Assembly. *Nano Lett.* **2004**, *4*, 1909–1914.
12. Cha, T.; Guo, A.; Jun, Y.; Pei, D.; Zhu, X. Y. Immobilization of Oriented Protein Molecules on Poly(ethylene glycol)-Coated Si(111). *Proteomics* **2004**, *4*, 1965–1976.
13. Lee, J. K.; Kim, Y. G.; Chi, Y. S.; Yun, W. S.; Choi, I. S. Grafting Nitrilotriacetic Groups onto Carboxylic Acid-Terminated Self-Assembled Monolayers on Gold Surfaces for Immobilization of Histidine-Tagged Proteins. *J. Phys. Chem. B* **2004**, *108*, 7665–7673.
14. Pasche, S.; De Paul, S. M.; Voeroes, J.; Spencer, N. D.; Textor, M. Poly(L-lysine)-graft-poly(ethylene glycol) Assembled Monolayers on Niobium Oxide Surfaces: A Quantitative Study of The Influence of Polymer Interfacial Architecture on Resistance to Protein Adsorption by ToF-SIMS and *in Situ* OWLSu OWLS. *Langmuir* **2003**, *19*, 9216–9225.
15. Huang, N. P.; Voeroes, J.; De Paul, S. M.; Textor, M.; Spencer, N. D. Biotin-Derivatized Poly(L-lysine)-g-poly(ethylene glycol): A Novel Polymeric Interface for Bioaffinity Sensing. *Langmuir* **2002**, *18*, 220–230.
16. Huang, N. P.; Michel, R.; Voros, J.; Textor, M.; Hofer, R.; Rossi, A.; Elbert, D. L.; Hubbell, J. A.; Spencer, N. D. Poly(L-lysine)-g-poly(ethylene glycol) Layers on Metal Oxide Surfaces: Surface-Analytical Characterization and Resistance to Serum and Fibrinogen Adsorption. *Langmuir* **2001**, *17*, 489–498.
17. Flynn, N. T.; Tran, T. N. T.; Cima, M. J.; Langer, R. Long-Term Stability of Self-Assembled Monolayers in Biological Media. *Langmuir* **2003**, *19*, 10909–10915.
18. Raynor, J. E.; Petrie, T. A.; Garcia, A. J.; Collard, D. M. Controlling Cell Adhesion to Titanium: Functionalization Of Poly[oligo(ethylene glycol)methacrylate] Brushes With Cell-Adhesive Peptides. *Adv. Mater.* **2007**, *19*, 1724–1728.
19. Faragher, R. J.; Schwan, A. L. New Deuterated Oligo(ethylene glycol) Building Blocks and Their Use in the Preparation of Surface Active Lipids Possessing Labeled Hydrophilic Tethers. *J. Org. Chem.* **2008**, *73*, 1371–1378.
20. Herrwerth, S.; Eck, W.; Reinhardt, S.; Grunze, M. Factors That Determine the Protein Resistance of Oligoether Self-Assembled Monolayers - Internal Hydrophilicity, Terminal Hydrophilicity, and Lateral Packing Density. *J. Am. Chem. Soc.* **2003**, *125*, 9359–9366.
21. Schwendel, D.; Dahint, R.; Herrwerth, S.; Schloerholz, M.; Eck, W.; Grunze, M. Temperature Dependence of the Protein Resistance of Poly- and Oligo(ethylene glycol)-Terminated Alkanethiolate Monolayers. *Langmuir* **2001**, *17*, 5717–5720.
22. Khademhosseini, A.; Jon, S.; Suh, K. Y.; Tran, T. N. T.; Eng, G.; Yeh, J.; Seong, J.; Langer, R. Direct Patterning of Protein- and Cell-Resistant Polymeric Monolayers and Microstructures. *Adv. Mater.* **2003**, *15*, 1995–2000.
23. Wang, R. L. C.; Kreuzer, H. J.; Grunze, M. Molecular Conformation and Solvation of Oligo(ethylene glycol)-Terminated Self-Assembled Monolayers and their Resistance to Protein Adsorption. *J. Phys. Chem. B* **1997**, *101*, 9767–9773.
24. Wang, R. L. C.; Kreuzer, H. J.; Grunze, M. The Interaction of Oligo(ethylene oxide) With Water: A Quantum Mechanical Study. *Phys. Chem. Chem. Phys.* **2000**, *2*, 3613–3622.
25. Ionov, L.; Stamm, M.; Diez, S. Size Sorting of Protein Assemblies Using Polymeric Gradient Surfaces. *Nano Lett.* **2005**, *5*, 1910–1914.
26. Karlstrom, G. A New Model for Upper and Lower Critical Solution Temperatures in Poly(ethylene oxide) Solutions. *J. Phys. Chem.* **1985**, *89*, 4962–4964.
27. Smith, G. D.; Bedrov, D. Roles of Enthalpy, Entropy, and Hydrogen Bonding in the Lower Critical Solution Temperature Behavior of Poly(ethylene oxide)/Water Solutions. *J. Phys. Chem. B* **2003**, *107*, 3095–3097.

28. Dormidontova, E. E. Influence of End Groups on Phase Behavior and Properties of PEO in Aqueous Solutions. *Macromolecules* **2004**, *37*, 7747–7761.
29. Balamurugan, S.; Ista, L. K.; Yan, J.; Lopez, G. P.; Fick, J.; Himmelhaus, M.; Grunze, M. Reversible Protein Adsorption and Bioadhesion on Monolayers Terminated With Mixtures of Oligo(ethylene glycol) and Methyl Groups. *J. Am. Chem. Soc.* **2005**, *127*, 14548–14549.
30. Cunliffe, D.; de Alarcon, C.; Peters, V.; Smith, J. R.; Alexander, C. Thermoresponsive Surface-Grafted Poly(*N*-isopropylacrylamide) Copolymers: Effect of Phase Transitions on Protein and Bacterial Attachment. *Langmuir* **2003**, *19*, 2888–2899.
31. Park, E. J.; Draper, D. D.; Flynn, N. T. Adsorption and Thermoresponsive Behavior of Poly(*N*-isopropylacrylamide-co-*N*,*N*′-cystaminebisacrylamide) Thin Films on Gold. *Langmuir* **2007**, *23*, 7083–7089.
32. Pong, F. Y.; Lee, M.; Bell, J. R.; Flynn, N. T. Thermo Responsive Behavior of Poly(*N*-isopropylacrylamide) Hydrogels Containing Gold Nanostructures. *Langmuir* **2006**, *22*, 3851–3857.
33. Cho, E. C.; Kim, Y. D.; Cho, K. Thermally Responsive Poly(*N*-isopropylacrylamide) Monolayer on Gold: Synthesis, Surface Characterization, and Protein Interaction/Adsorption Studies. *Polymer* **2004**, *45*, 3195–3204.
34. Zhu, M. Q.; Wang, L. Q.; Exarhos, G. J.; Li, A. D. Q. Thermo Sensitive Gold Nanoparticles. *J. Am. Chem. Soc.* **2004**, *126*, 2656–2657.
35. Jones, D. M.; Smith, J. R.; Huck, W. T. S.; Alexander, C. Variable Adhesion of Micropatterned Thermoresponsive Polymer Brushes: AFM Investigations of Poly(*N*-isopropylacrylamide) Brushes Prepared by Surface-Initiated Polymerizations. *Adv. Mater.* **2002**, *14*, 1130–1134.
36. Cheng, X.; Canavan, H. E.; Graham, D. J.; Castner, D. G.; Ratner, B. D. Temperature-dependent Activity and Structure of Adsorbed Proteins on Plasma Polymerized *N*-Isopropyl Acrylamide. *Biointerphases* **2006**, *1*, 61–72.
37. Valkama, S.; Kosonen, H.; Ruokolainen, J.; Haatainen, T.; Torkkeli, M.; Serimaa, R.; ten Brinke, G.; Ikkala, O. Self-assembled Polymeric Solid Films With Temperature-Induced Large and Reversible Photonic-Bandgap Switching. *Nat. Mater.* **2004**, *3*, 872–876.
38. Hyun, J.; Lee, W. K.; Nath, N.; Chilkoti, A.; Zauscher, S. Capture and Release of Proteins on the Nanoscale by Stimuli-Responsive Elastin-Like Polypeptide "Switches". *J. Am. Chem. Soc.* **2004**, *126*, 7330–7335.
39. Mather, P. T. Responsive Materials: Soft Answers for Hard Problems. *Nat. Mater.* **2007**, *6*, 93–94.
40. Dexter, A. F.; Malcolm, A. S.; Middelberg, A. P. J. Reversible Active Switching of the Mechanical Properties of a Peptide Film at a Fluid-Fluid Interface. *Nat. Mater.* **2006**, *5*, 502–506.
41. Boyer, C.; Bulmus, V.; Liu, J.; Davis, T. P.; Stenzel, M. H.; Barner-Kowollik, C. Well-Defined Protein-Polymer Conjugates *Via In-Situ* RAFT Polymerization. *J. Am. Chem. Soc.* **2007**, *129*, 7145–7154.
42. Lutz, J. F.; Akdemir, A.; Hoth, A. Point by Point Comparison of Two Thermosensitive Polymers Exhibiting a Similar LCST: Is the Age of Poly(NIPAM) Over. *J. Am. Chem. Soc.* **2006**, *128*, 13046–13047.
43. Fundueanu, G.; Constantin, M.; Bortolotti, F.; Cortesi, R.; Ascenzi, P.; Menegatti, E. Poly[(*N*-isopropylacrylamide-co-acrylamide-co-(hydroxyethylmethacrylate))] Thermoresponsive Microspheres: An Accurate Method Based on Solute Exclusion Technique To Determine the Volume Phase Transition Temperature. *Eur. Polym. J.* **2007**, *43*, 3500–3509.
44. Feil, H.; Bae, Y. H.; Feijen, J.; Kim, S. W. Effect of Comonomer Hydrophilicity and Ionization on the Lower Critical Solution Temperature of N-Isopropylacrylamide Copolymers. *Macromolecules* **1993**, *26*, 2496–2500.
45. Kosik, K.; Wilk, E.; Geissler, E.; Laszlo, K. Influence of a Crown Ether Comonomer on the Temperature-Induced Phase Transition of Poly(*N*-isopropylacrylamide) Hydrogels. *J. Phys. Chem. B* **2008**, *112*, 1065–1070.
46. Francis, R.; Jijil, C. P.; Prabhu, C. A.; Suresh, C. H. Synthesis of Poly(*N*-isopropylacrylamide) Copolymer Containing Anhydride and Imide Comonomers- A Theoretical Study on Reversal Of LCST. *Polymer* **2007**, *48*, 6707–6718.
47. Dimitrov, I.; Trzebicka, B.; Mueller, A. H. E.; Dworak, A.; Tsvetanov, C. B. Thermosensitive Water-Soluble Copolymers with Doubly Responsive Reversibly Interacting Entities. *Prog. Polym. Sci.* **2007**, *32*, 1275–1343.
48. Biacore 2000 Handbook, version AB; Biacore: Uppsala, Sweden, 1998.
49. Jungs, L. S.; Campbell, C. T.; Chinowsky, T. M.; Mar, M. N.; Sinclair, S. Y. Quantitative Interpretation of the Response of Surface Plasmon Resonance Sensors to Adsorbed Films. *Langmuir* **1998**, *14*, 5636–5648.
50. Ulman, A. Formation and Structure of Self-Assembled Monolayers. *Chem. Rev.* **1996**, *96*, 1533–1554.
51. Cao, R., Jr.; Díaz, A.; Cao, R.; Otero, A.; Cea, R.; Rodríguez-Argüelles, M. C.; Serra, C. Building Layer-By-Layer a Bis(dithiocarbamato)copper(II) Complex on Au{111} Surfaces. *J. Am. Chem. Soc.* **2007**, *129*, 6927–6930.
52. Kocharova, N.; Aaritalo, T.; Leiro, J.; Kankare, J.; Lukkari, J. Aqueous Dispersion, Surface Thiolation, and Direct Self-Assembly of Carbon Nanotubes on Gold. *Langmuir* **2007**, *23*, 3363–3371.
53. Vance, A. L.; Willey, T. M.; Nelson, A. J.; van Buuren, T.; Bostedt, C.; Terminello, L. J.; Fox, G. A. XAS and XPS Characterization of Monolayers Derived From a Dithiol and Structurally Related Disulfide-Containing Polyamides. *Langmuir* **2002**, *18*, 8123–8128.
54. Chen, X.; Pelton, R. Pre-Adsorption of Amphiphilic Polymers on Synthetic Surfaces for Biofouling Retardation. *Adv. Mater. Res.* **2006**, *11−12*, 363–366.
55. Balamurugan, S.; Mendez, S.; Balamurugan, S. S.; O'Brien, M. J.; Lopez, G. P. Thermal Response Of Poly(*N*-isopropylacrylamide) Brushes Probed by Surface Plasmon Resonance. *Langmuir* **2003**, *7*, 2545–2549.
56. Nelson, K. E.; Gamble, L.; Jung, L. S.; Boeckl, M. S.; Naeemi, E.; Golledge, S. L.; Sasaki, T.; Castner, D. G.; Campbell, C. T.; Stayton, P. S. Surface Characterization of Mixed Self-Assembled Monolayers Designed for Streptavidin Immobilization. *Langmuir* **2001**, *17*, 2807–2816.
57. Jung, L. S.; Nelson, K. E.; Stayton, P. S.; Campbell, C. T. Binding and Dissociation Kinetics of Wild-Type and Mutant Streptavidins on Mixed Biotin-Containing Alkylthiolate Monolayers. *Langmuir* **2000**, *16*, 9421–9432.
58. Schwendel, D.; Dahint, R.; Herrwerth, S.; Schloerholz, M.; Eck, W.; Grunze, M. Temperature Dependence of the Protein Resistance of Poly- and Oligo(ethylene glycol)-terminated Alkanethiolate Monolayers. *Langmuir* **2001**, *17*, 5717–5720.
59. Peres-Luna, V. H.; O'Brien, M. J.; Opperman, K. A.; Hampton, P. D.; López, G. P.; Klumb, L. A.; Stayton, P. S. Molecular Recognition Between Genetically Engineered Streptavidin and Surface-bound Biotin. *J. Am. Chem. Soc.* **1999**, *121*, 6469–6478.
60. Xia, N.; Shumaker-Parry, J. S.; Zareie, M. H.; Campbell, C. T.; Castner, D. G. A Streptavidin Linker Layer That Functions After Drying. *Langmuir* **2004**, *20*, 3710–3716.
61. Waner, M. J.; Navrotskaya, I.; Bain, A.; Oldham, E. D.; Mascotti, D. P. Thermal and Sodium Dodecylsulfate Induced Transitions of Streptavidin. *Biophys. J.* **2004**, *87*, 2701–2713.
62. Gonzalez, M.; Argarana, C. E.; Fidelio, G. D. Extremely High Thermal Stability of Streptavidin and Avidin Upon Biotin Binding. *Biomol. Eng.* **1999**, *16*, 67–72.
63. Bayer, E. A.; Ehrligh-Rogozinski, S.; Wilchek, M. Sodium Dodecyl Sulfate-Polyacrylamide Gel Electrophoretic Method for Assessing the Quaternary State and Comparative Thermostability of Avidin and Streptavidin. *Electrophoresis* **1996**, *17*, 1319–1324.
64. Beamson, G.; Briggs, D. High Resolution XPS of Organic Polymers. *The Scienta ESCA300 Database;* Wiley Interscience: New York, 1992.